Available online at www.sciencedirect.com
ScienceDirect
Journal of Power Sources 165 (2007) 403–407
JOURNAL OF POWER SOURCES
www.elsevier.com/locate/jpowsour

Short communication

Effect of chemical oxidation for nano-size γ-Fe_2O_3 as lithium battery cathode

Sho Kanzaki, Atsuo Yamada, Ryoji Kanno *

Department of Electronic Chemistry, Interdisciplinary Graduate School of Science and Engineering, Tokyo Institute of Technology, 4259 Nagatsuta, Midori, Yokohama 226-8502, Japan

Received 22 November 2006; accepted 5 December 2006
Available online 12 January 2007

Abstract

Surface treatment of nano-crystalline γ-Fe_2O_3 was examined to improve its electrochemical performances for lithium battery. Removal of residual phases on the surface by chemical oxidation with NO_2BF_4 was confirmed by TG measurement and FT-IR spectroscopy, and the process improved charge–discharge characteristics; higher capacity and better reversibility were obtained. The charge–discharge mechanism was studied by X-ray diffraction measurement and Mössbauer spectroscopy. The reversible charge–discharge reaction of the nano-size γ-Fe_2O_3 was proceeded by a phase transition between the spinel and the disordered rock-salt type, which was previously claimed to be an irreversible process for the bulk materials. The nano-size effect of the phase transitions and the charge–discharge mechanism will be discussed.

Keywords: Iron oxide; Lithium battery electrode; Spinel-rocksalt transformation; Nano particle

1. Introduction

Iron based materials are one of the most ideal cathodes for lithium secondly batteries because of its low cost and low environmental impact, in comparison with cobalt or nickel based cathode materials containing heavy metals as an active reaction center. Many types of materials have been prepared, such as α-Fe_2O_3 [1–4], γ-Fe_2O_3 [5,6], Fe_3O_4 [7], $LiFeO_2$ [8–14], $LiFePO_4$ [15–19]. Among these materials, simple iron oxides, α-Fe_2O_3, Fe_3O_4 and γ-Fe_2O_3, have been considered to be difficult for the use of cathode materials, because the lithiation at the first discharge process caused a phase transition from the corundum/spinel to the disordered rock-salt type [5], and the extraction of lithium from the rock-salt phase was difficult due to the irreversible transition process. However, we recently proposed that the nano-particles of γ-Fe_2O_3 showed good reversibility for lithium battery cathode reaction.

The maghemite, γ-Fe_2O_3, has the spinel structure with iron occupying both tetrahedral and octahedral sites, and vacancy at the octahedral site. Although the spinel structure has been considered to be suitable for high lithium-ionic diffusion through the pathway between 8a tetrahedral – 16c interstitial octahedral – 8a tetrahedral sites, the iron situated at the tetrahedral site blocks the lithium ion diffusion in γ-Fe_2O_3, thus leading to poor cathode characteristics. The γ-Fe_2O_3 showed an irreversible transformation from the spinel to the rock-salt structure accompanied by the lithiation process, which caused low cycling characteristics for lithium battery electrodes. In order to overcome the irreversible characteristics, we synthesized nano-size γ-Fe_2O_3 and clarified its electrochemical properties [20]. We found that the irreversible phase transformation was suppressed for the nano-size materials, and the reversible lithium intercalation and de-intercalation proceeded by a topochemical reaction. However, only a low reversible capacity was observed, although relatively a large value of 230 mAh g^{-1} was obtained for the first discharge capacity.

There are several possibilities that caused low reversible characteristics. (i) Protons adsorbed on the surface of the particles react with lithium. (ii) Lithium insertion and extraction reactions caused aggregation of nano-size particles, which provided drastic degradation of reversibility. (iii) Impurity phases still exist on the nano-particle surface, which were deposited during the synthesis process, and the surface purification treatment was not efficient to remove these phases. We supposed that the surface

* Corresponding author.
E-mail address: kanno@echem.titech.ac.jp (R. Kanno).

0378-7753/$ – see front matter © 2007 Elsevier B.V. All rights reserved.
doi:10.1016/j.jpowsour.2006.12.001

protons or impurity phases might be the main reasons for its low reversible characteristics, because the particles had very small size (under 8 nm) and large surface area (140 $m^2\,g^{-1}$) without any morphology changes after the lithiation experiments.

In the present study, the effect of chemical oxidation for nano-size γ-Fe_2O_3 was examined. The nano-particles synthesized by the Hyeon's method [21] were treated by chemical oxidation using NO_2BF_4. The electrochemical properties examined for γ-Fe_2O_3 after the oxidation process provided better cycling characteristics with reversible phase transition between the spinel and the rock-salt structures, which was previously claimed to be irreversible process.

2. Experimental

Nano-size γ-Fe_2O_3 was synthesized by mild oxidation of $Fe(CO)_5$ using a method reported previously [21]. $Fe(CO)_5$ (1.0 ml) was added to a mixture of 50 ml of octylether and 2.4 ml of oleic acid, used as surfactant, at 100 °C. The solution was refluxed for 1 h. After cooling to room temperature, 1.7 g of dehydrated trimethylamin *N*-oxide as oxidant was added. The solution was heated again to 130 °C and the temperature was kept for 2 h. Then, the reaction temperature was slowly increased up to the reflux point, and was kept for 1 h. All the processes were performed in an Ar atmosphere. After cooling to room temperature, excess ethanol was added. The black precipitate was centrifuged for isolation, and washed with ethanol. The products obtained were heat treated at 150 °C for 20 h in an oxygen atmosphere to remove impurity phases on the surface.

The chemical oxidation was carried out at room temperature. The iron oxides were stirred with NO_2BF_4 in an acetonitrile for 24 h in an inert atmosphere of Ar gas flow. After the reaction, the precipitate was centrifuged for isolation, washed with acetonitrile to remove oxidant and the other products, and dried in a vacuum at 60 °C for one night. These samples were characterized by scanning electron microscopy (Hitachi Co., S-4800), FT-IR spectroscopy (NICOLET, NEXUS 670 FT-IR), X-ray diffraction (XRD) measurement (Rigaku, RU-200, 12 kW) with an Cu Kα radiation, and TG-DTA measurement (SII, TG/DTA6300, EXSTAR6000) with a heating rate of 5 °C min^{-1} up to 500 °C in air.

Electrochemical characteristics of the nano-particles were measured at 25 °C with a 2032 coin type cell or a test cell (Hohsen Co.) with lithium metal as an anode. The electrolyte was ethylene carbonate (EC)–diethyl carbonate (DEC) with a molar ratio of 3:7 as a solvent and a supporting electrolyte of 1 M $LiPF_6$. The cathode was a mixture of γ-Fe_2O_3:acetylene black:poly(vinilidene fluoride) (PVdF), with a weight ratio of 4:2:1. The mixture was dispersed into *N*-methyl-2-pyrrolidinone (NMP), and the slurry was cast on an Al foil to form an electrode. The electrode was dried at 80 °C in a vacuum before supplying for electrochemical tests.

3. Results and discussion

Chemical oxidation is one of the effective techniques of diprotonation and to remove residual impurity phases. We chose

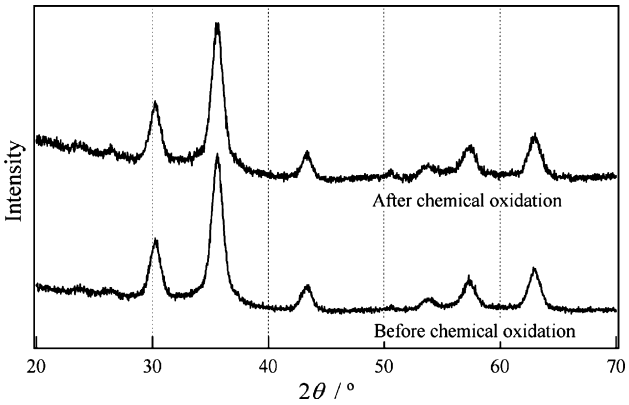

Fig. 1. XRD patterns of nano-size γ-Fe_2O_3, before (bottom) and after (top) chemical oxidation.

NO_2BF_4 as an oxidant and acetonitrile as an aprotic solvent. NO_2BF_4 is a strong oxidant with an oxidation potential higher than 5 V, which is efficient to obtain high-oxidized materials [22]. The nano-particles of γ-Fe_2O_3 were treated with the chemical oxidation. Fig. 1 shows the XRD patterns of nano-size γ-Fe_2O_3 before and after the chemical oxidation. No significant change was found in the diffraction patterns with the chemical oxidation. The lattice parameters were calculated to be $a = 8.3472(6)$ and $8.3472(7)$ Å for the samples before and after the oxidation, respectively, indicating no changes in the bulk structure with the chemical oxidation process. Fig. 2 shows SEM images of the nano-size γ-Fe_2O_3 before and after the chemical oxidation process. No morphology change with the chemical treatment was confirmed. These results indicate that the chemical oxidation process caused no influence on the structures, particle size, and morphology of γ-Fe_2O_3. Fig. 3 shows the TG curves of nano-size γ-Fe_2O_3 before and after the chemical oxidation together with the sample after immersed in acetonitrile. A weight loss of 9 wt.% was observed for the sample before chemical oxidation and treated with acetonitrile. As the samples treated with NO_2BF_4 showed a weight loss of about 6 wt.%, about 3 wt.% of residual impurity phase was removed by the oxidation.

The TG measurements indicated that the phase synthesized by the Hyeon's method contained an impurity phase which could be removed both by thermal treatment and the chemical oxidation process. In order to characterize the impurity phase, the phase was tried to be extracted from the coarse products by bulb-to-bulb distillation using Kugelrohr (Aldrich Co.) at 220 °C under vacuum condition [23]. The composition analysis of the extracted product using FT-IR, TG-MS, ^1H NMR and ^{13}C NMR suggests that the phase was composed of a mixture of macromolecule compounds, such as dimer of oleic acid, amide compounds made from oleic acid and trimethylamin *N*-oxide. However, the precise composition was not able to be determined. Fig. 4 shows the FT-IR spectra of nano-size γ-Fe_2O_3 before and after the chemical oxidation process, and a residual phase extracted by the distillation process. The IR spectra showed peaks around 2900 cm^{-1} characteristic of the residual impurity phase. After the chemical oxidation, these peaks disappeared for the nano-size γ-Fe_2O_3, indicating that the surface impurity

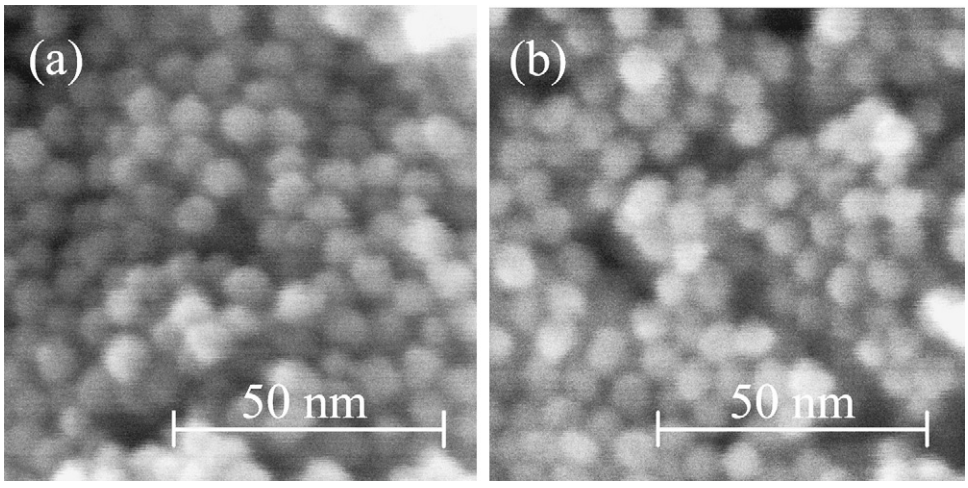

Fig. 2. SEM images of γ-Fe_2O_3, before (a) and after (b) chemical oxidation. Magnification: ×800,000.

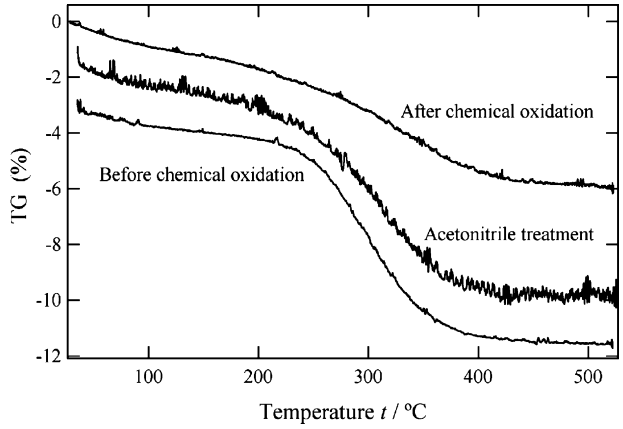

Fig. 3. TG curves of nano-size γ-Fe_2O_3, before chemical oxidation (bottom), after chemical oxidation (top) and after immersed in acetonitrile solution. For clarity, the data for acetonitrile treatment and before chemical oxidation are offset 1 and 3%, respectively.

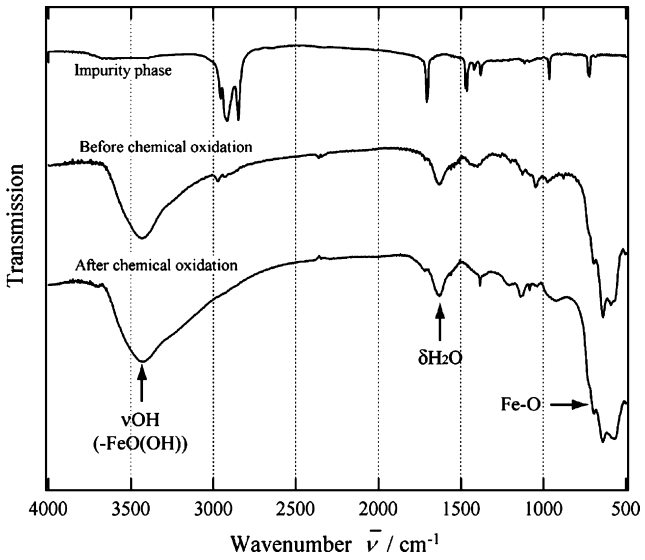

Fig. 4. FT-IR spectrum for nano-size γ-Fe_2O_3, before chemical oxidation (middle), after chemical oxidation (bottom), and the impurity phase extracted by evaporation method (top). Impurity phase was observed for the sample before chemical oxidation.

phase was removed by the chemical oxidation treatment. On the other hand, no significant changes were observed for the peaks around 1380 and 1640, and 3400 cm^{-1}, which correspond to H_2O, and −O(OH) on the surface, respectively. These results indicate that the chemical oxidation was efficient to remove the impurity phase on the surface of nano-size γ-Fe_2O_3 particles, but the process was not efficient to remove protons which were adsorbed or chemically bonded on the surface.

Fig. 5 shows the first discharge curves of the nano-size γ-Fe_2O_3 before and after the chemical oxidation process. The cut-off voltage was 1.0 V. The discharge capacities of 200 mAh g^{-1} for the sample before chemical oxidation increased to 236 mAh g^{-1} after the treatment; about 18% of its discharge capacity was increased with the chemical oxidation process. Fig. 6 shows the ex situ XRD patterns of the chemically oxidized γ-Fe_2O_3 and the lithiated γ-Fe_2O_3. The XRD patterns of the lithiated γ-Fe_2O_3 were measured for the samples after discharged to a fixed voltage (2.0–1.0 V in the figure), and the sample after charged from 1.0 to 4.0 V (4.0 V in the figure). During the discharge process above 1.2 V, no significant changes in the diffraction patterns were observed; only a slight peak shift to the lower angles was found. For the sam-

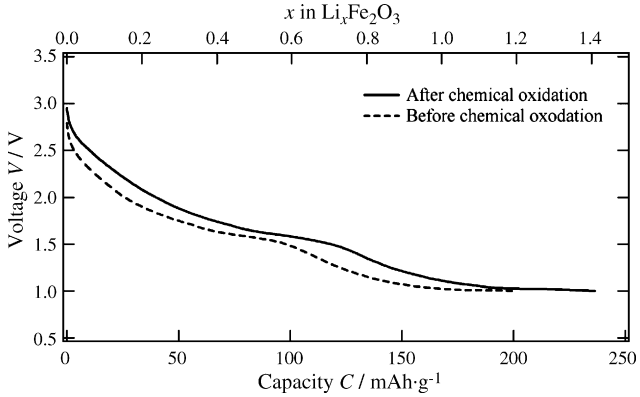

Fig. 5. First discharge curves for nano-size γ-Fe_2O_3 before chemical oxidation process (dotted line) and after chemical oxidation process (solid line). Conditions: cut-off voltage, 1.0 V; current density, 50 μA cm^{-2}.

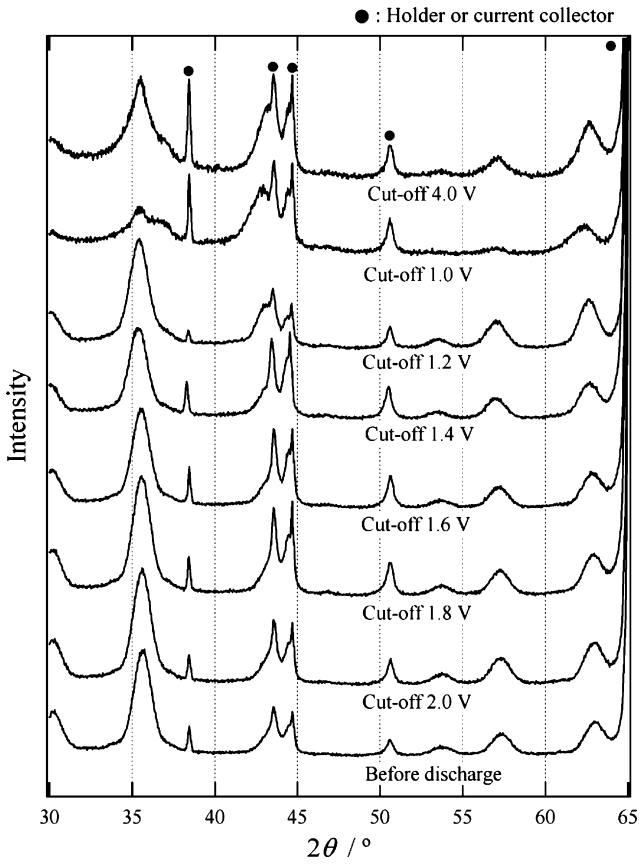

Fig. 6. XRD patterns of nano-size γ-Fe_2O_3, before and after the discharge process. The mark (●) indicates the current collector or XRD holder.

ple discharged to 1.0 V, new peaks appeared around $2\theta = 37^\circ$ and 43° attributed to the disordered-rock-salt phase, which indicates a phase transformation from the spinel to the disordered rock-salt phase. We reported previously that the irreversible spinel-rocksalt phase transformation was suppressed by making nano-particles, while the micro-size particles showed the irreversible spinel-rocksalt phase transition [20]. However, a larger amount of lithium inserted into the nano-particles by the surface treatment of chemical oxidation caused a phase transformation from the spinel to the rock-salt type. The amount of the rock-salt phase produced from the spinel structure was estimated by fitting XRD patterns with the Rietveld method [24]; a ratio of the spinel/rock-salt phase was determined to be 0.2/0.8. The fitting pattern of the sample discharged to 1.0 V is shown in Fig. 7.

Fig. 8 shows Mössbauer spectra of the nano-size γ-Fe_2O_3 before and after the discharge processes. The nano-size γ-Fe_2O_3 before discharge showed the existence of Fe(III), while a mixed valence state was observed with a ratio of Fe(III)/Fe(II) = 57/43 after the discharge. Bonnet et al. [5] reported that the transformation from the spinel to the disordered rock-salt phase proceeded when the amount of 0.87 Li was reacted with γ-Fe_2O_3 in the bulk crystalline materials. Assuming that the lithium content of the rock-salt phase was 0.87, the composition of the spinel phase was calculated to be $Li_{0.82}Fe_2O_3$ using the amount of spinel/rock-salt phase ratio and the Fe(III)/Fe(II) ratio determined by XRD and Mössbauer spectroscopy, respectively. The

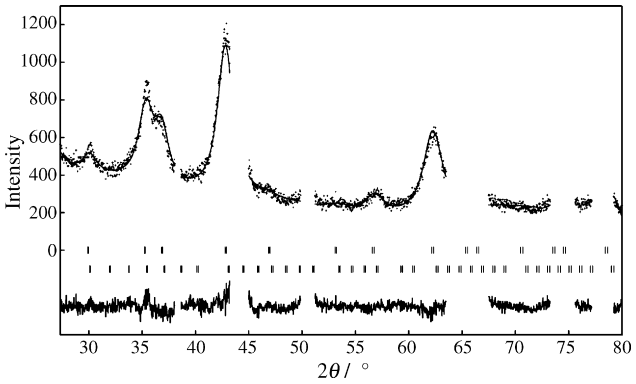

Fig. 7. Rietveld refinement pattern of lithiated γ-Fe_2O_3 to a cut-off voltage of 1.0 V. The diffraction angles near the peaks due to current corrector and diffraction holders were excluded from the calculation.

XRD pattern fitting analysis for the sample after charge to 4.0 V provided a spinel/rock-salt ratio of 0.5/0.5, clearly indicating that the disordered rock-salt phase transformed again to the spinel structure with the charge process; the reversible spinel/rock-salt transformation was found for our ultra fine nano-particles.

Fig. 9a shows charge–discharge curves of the nano-size γ-Fe_2O_3 after the chemical oxidation with a current density of 50 μA cm^{-2} (about 0.7 C rate) and cut-off voltages of 1.0 and 4.0 V for the discharge and charge, respectively. Fig. 9b shows the cycling characteristics of γ-Fe_2O_3 before and after the chemical oxidation. The chemical treatment improved the cycling characteristics. However, a large irreversible capacity was still observed; a reaction between lithium and the surface caused an irreversible reaction. The irreversible capacity was about 75.3 mAh g^{-1}, which corresponds to the nominal composition of 0.45 Li for γ-Fe_2O_3.

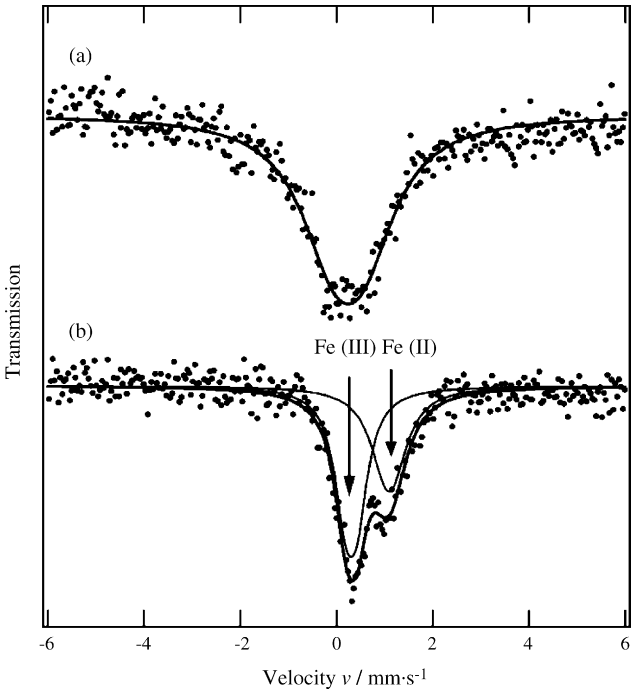

Fig. 8. Mössbauer spectra of nano-size γ-Fe_2O_3. Initial state (a) and after discharge process (b) down to 1.0 V vs. Li/Li^+.

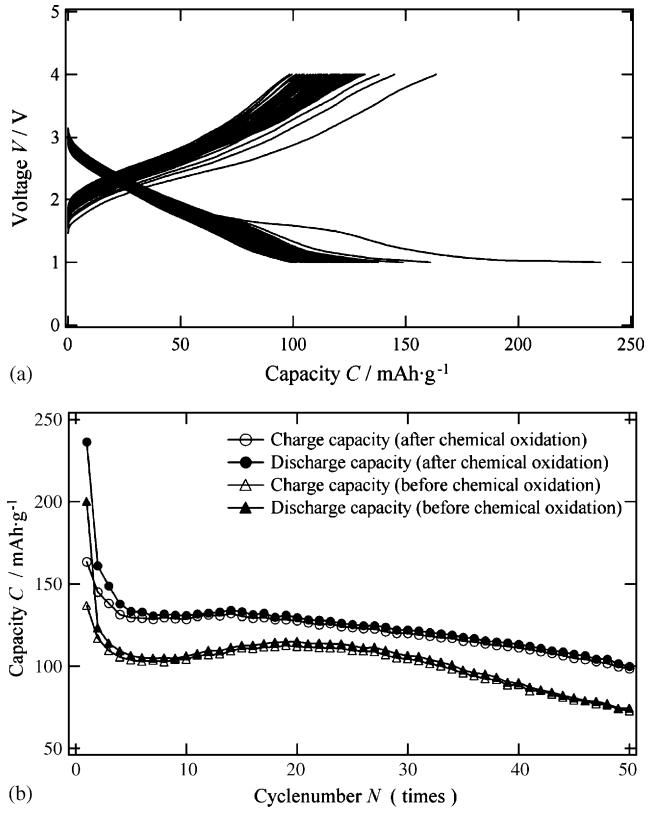

Fig. 9. (a) Charge–discharge curves of nano-size γ-Fe_2O_3. Conditions: cut-off voltage: 1.0 and 4.0 V; current density: 50 μA cm^{-2}. (b) Cycle number dependence of charge–discharge capacities of nano-size γ-Fe_2O_3 before and after chemical oxidation process.

In the present study, we indicated the importance of surface conditions and phase transition mechanism of the nano-particles for electrochemical reactions. As the nano-particles provided large surface area, the control of the surface conditions is very important for the electrochemical characteristics. The main impurity phase formed during the synthesis process was successfully removed by our chemical treatment, and the reversible lithium capacity was improved. However, the FT-IR and TG characterization of the nano-particles indicated that there are still residual protons on the surface, and the surface condition of the nano-particles was found to be an important factor that determines both the capacity and reversibility of electrode characteristics. We also confirmed the reversible spinel/rock-salt phase transition for the nano-particles, although a complete phase change was not observed during the first charge–discharge cycle for our present samples. Reversible phase transition with the lithium (de)intercalation into the γ-Fe_2O_3-type spinel structure may indicate further possibility to improve reversible capacities of the nano-particles.

4. Conclusion

We investigated the effect of chemical oxidation with NO_2BF_4 for nano-size γ-Fe_2O_3. The chemical oxidation removed the residual impurity phase without any changes in particle size and morphology of the nano-particles. The sample after chemical oxidation showed larger charge–discharge capacity with better cycling characteristics. The increase in the amount of lithium intercalated into the structure (discharge capacity) caused a phase change from the spinel to the rock-salt structure. However, the reversible behavior of the spinel/rock-salt phase transition may indicate a possibility of capacity increase in the spinel-type iron oxides. The chemical oxidation process is efficient to improve electrochemical characteristics of nano-particles with high surface area. However, large surface area of the nano-particles affects the electrochemical properties and the control of the surface conditions is an important factor to improve the capacity.

Acknowledgement

The authors thank Dr. Takanobu Sanji and Dr. Taro Inada for the analysis by NMR and TG-MS measurements. We thank Dr. Yoshikazu Kumashiro for the help of FT-IR measurements.

References

[1] M.M. Thackeray, W.I.F. David, J.B. Goodenough, Mater. Res. Bull. 17 (1982) 785.
[2] S. Komaba, K. Suzuki, N. Kumagai, Electrochemistry 70 (2002) 506.
[3] D. Larcher, D. Bonnin, R. Cortes, I. Rivals, L. Personnaz, J.M. Tarascon, J. Electrochem. Soc. 150 (2003) A1643.
[4] D. Larcher, C. Masquelier, D. Bonnin, Y. Chabre, V. Masson, J.B. Leriche, J.M. Tarascon, J. Electrochem. Soc. 150 (2003) A133.
[5] B. Bonnet, P. Strobel, M. Pernet, M. Gondrand, Y. Gros, C. Mouget, Y. Chabre, Mater. Sci. Forum 91–93 (1992) 345.
[6] M. Pernet, P. Strobel, B. Bonnet, P. Bordet, Y. Chabre, Solid State Ionics 66 (1993) 259.
[7] M.S. Islam, C.R.A. Catlow, J. Solid State Chem. 77 (1988) 180.
[8] N. Imanishi, K. Nakahara, Y. Takeda, O. Yamamoto, M. Takano, Denki Kagaku 61 (1993) 1451.
[9] R. Kanno, T. Shirane, Y. Kawamoto, Y. Takeda, M. Takano, M. Ohashi, Y. Yamaguchi, J. Electrochem. Soc. 143 (1996) 2435.
[10] K. Ado, M. Tabuchi, H. Kobayashi, H. Kageyama, O. Nakamura, Y. Inaba, R. Kanno, M. Takagi, Y. Takeda, J. Electrochem. Soc. 144 (1997) L177.
[11] Y. Sakurai, H. Arai, S. Okada, J.-i. Yamaki, J. Power Sources 68 (1997) 711.
[12] T. Matsumura, R. Kanno, Y. Inaba, Y. Kawamoto, M. Takano, J. Electrochem. Soc. 149 (2002) A1509.
[13] Y.S. Lee, S. Sato, Y.K. Sun, K. Kobayakawa, Y. Sato, J. Power Sources 119–121 (2003) 285.
[14] Y.S. Lee, S. Sato, M. Tabuchi, C.S. Yoon, Y.K. Sun, K. Kobayakawa, Y. Sato, Electrochem. Commun. 5 (2003) 549.
[15] A.K. Padhi, K.S. Nanjundaswamy, J.B. Goodenough, J. Electrochem. Soc. 144 (1997) 1188.
[16] S. Okada, S. Sawa, M. Egashira, J.-i. Yamaki, M. Tabuchi, H. Kageyama, T. Konishi, A. Yoshino, J. Power Sources 97–98 (2001) 430.
[17] A. Yamada, M. Hosoya, S.C. Chung, K. Hinokuma, Y. Kudo, K.Y. Liu, Ceram. Trans. 127 (2002) 189.
[18] A. Yamada, M. Hosoya, S.-C. Chung, Y. Kudo, K. Hinokuma, K.-Y. Liu, Y. Nishi, J. Power Sources 119–121 (2003) 232.
[19] A. Yamada, H. Koizumi, S.-I. Nishimura, N. Sonoyama, R. Kanno, M. Yonemura, T. Nakamura, Y. Kobayashi, Nat. Mater. 5 (2006) 357.
[20] S. Kanzaki, T. Inada, T. Matsumura, N. Sonoyama, A. Yamada, M. Takano, R. Kanno, J. Power Sources 146 (2005) 323.
[21] T. Hyeon, S.S. Lee, J. Park, Y. Chung, H.B. Na, J. Am. Chem. Soc. 123 (2001) 12798.
[22] A.R. Wizansky, P.E. Rauch, F.J. Disalvo, J. Solid State Chem. 81 (1989) 203.
[23] R. Graeve, G.H. Wahl, J. Chem. Educ. 41 (1964) 279.
[24] F. Izumi, T. Ikeda, Mater. Sci. Forum 198 (2000) 321.